J. Quant. Spectrosc. Radiat. Transfer Vol. 41, No. 2, pp. 93–96, 1989
Printed in Great Britain.

0022-4073/89 $3.00 + 0.00

EFFECT OF POWER VARIATION ON THERMAL PLASMA OPTICAL DIAGNOSTIC DATA

VIVEK BAKSHI and R. J. KEARNEY
Department of Physics, University of Idaho, Moscow, ID 83843, U.S.A.

(*Received* 31 *May* 1988)

Abstract—The effect of sinusoidal power variations on emissivity and line-shape measurements of Ar I transitions and the H_β transition are examined, both by a computer simulation and with experiments. The average over substantial power variation (20–50%) for both total emissivity and transition half-width data is shown to agree, within data-processing errors, with results obtained from pure d.c. operation.

INTRODUCTION

Optical spectroscopy measurements have been extensively used for thermal plasma diagnostics experiments. In order to interpret the experimental data, a common assumption is that the power supplied to the plasma device does not vary in time. In practice, this is often not a good assumption. Commercial power supplies with currents of the order of 200–1000 A are typically saturated core power supplies with an appreciable 180 or 360 Hz power variation. Even with well-filtered outputs and d.c. power supplies, plasma arc dynamics may cause time variation in the power delivered to the plasma system.[1] In this paper, we examine the effect of sinusoidal power variation on emissivity and line-shape measurements of Ar I transitions and on the line shape of the H_β line.

THEORETICAL ANALYSIS

We consider a plasma experiment with measurements of intensity taken side-on, as shown in Fig. 1. To obtain intensity in radial space, we use the Abel-inversion technique. We consider thermal plasma regions for which the electron density is in the range of $1–10 \times 10^{22}$ m^{-3}. In these situations, the dominant mechanism for line broadening of isolated neutral atoms is collisions with electrons.[2–5] For non-hydrogenic atoms the impact theory gives the resultant line shape as a symmetric Lorentzian profile.[3–5]

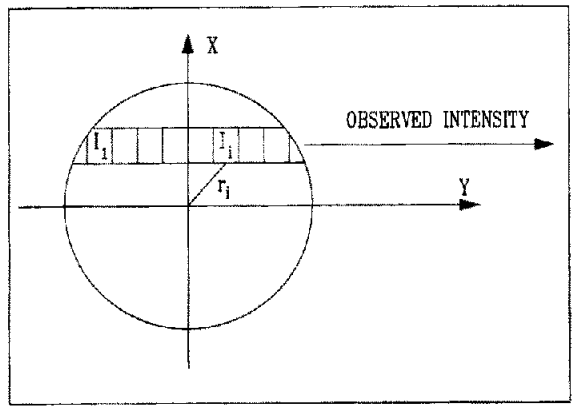

Fig. 1. Radial cross-section of the plasma jet is shown. For a given X, the distribution in Y is subdivided into N cells, each having a characteristic intensity I_i. The observed intensity is the sum of the intensities from all of these cells at a given X position.

As shown in Fig. 1, for a given X, the distribution in Y is subdivided into N cells, each having a characteristic emissivity I_i described by the relation

$$I_i = I(\sqrt{X^2 + Y_i^2}) = I(r_i).$$

The normalized side-on intensity $I(\lambda, X)$ is considered to be an average of Lorentzian contributions

$$I(\lambda, X) = \left[\frac{1}{N}\right] \sum_{i=1}^{N} I_i L(\Gamma_i, \lambda). \tag{1}$$

Here,

$$L(\Gamma_i, \lambda) = \left[\frac{1}{2\pi}\right]\left[\frac{\Gamma_i}{(\lambda - \lambda_0)^2 + (\Gamma_i/2)^2}\right] \tag{2}$$

is the normalized Lorentzian. The peak wavelength of the transition is represented by λ_0 and Γ_i is the half-width. Equations (1) and (2) represent the d.c. case where I_i is constant in time. If, however, I_i varies in a periodic fashion and we average over the entire period, the side-on intensity becomes

$$\overline{I(\lambda, X)} = \left[\frac{1}{N}\right] \sum_{i=1}^{N} \overline{I_i L(\Gamma_i, \lambda)}, \tag{3}$$

where

$$\overline{I_i L(\Gamma i, \lambda)} = \left[\frac{1}{P}\right] \sum_{j=1}^{P} \overline{I_i(t_j)\, L(\Gamma_j, \lambda)}, \tag{4}$$

and the sum over j averages the power variation. The total intensity in a cell is now $I_i(t_j)$. We consider a sine variation for I_j at a general cell since any periodic variation can be represented as a sum of sine variations. If on a normal scale $\langle I_j \rangle = 1$, then we take

$$I_i(t_j) = 1 + 0.5 \sin(2\pi t_j / T), \tag{5}$$

where T is the time period of the sinusoidal variation. In many cases, there is only one dominant period and this equation is a good approximation to the emissivity. Equation (5) corresponds to 50% variation in the intensity I_j.

As a starting point for our analysis, we need to generate the intensities $I_1 \ldots I_i$ in Fig. 1. In order to do this, we start with an $I(r)$ vs r curve (we have taken an experimentally-determined distribution for the 8265 Å Ar I transition[6]) and generate $I_1 \ldots I_i \ldots$ for a given X, for 100 i values. Then we calculate both $I(\lambda, X)$ and $\overline{I(\lambda, X)}$. In order to perform these calculations, we need to know the variation of Γ_i with I_i and use the following relation:[3]

$$\Gamma = 2[1 + 1.75 \times 10^{-4} N_e^{1/4} \alpha (1 - 0.068\, N_e^{1/6} T^{1/6})]\, 10^{-16}\, W N_e. \tag{6}$$

The electron-impact parameter W and the ion-broadening parameter α are tabulated[5] and the intensity I_i, electron density N_e, and temperature T are related through equations assuming local thermodynamic equilibrium (LTE).[6] We have generated $I(\lambda, X)$ and $\overline{I(\lambda, X)}$ for X values from 0 to R (R is the radius of the plasma jet and is about 3.5 mm in our experiments) for 100 $\lambda - \lambda_0$ values. Individual values of $I(\lambda, X_i)$ and $\overline{I(\lambda, X_i)}$ show differences which vary from $<1\%$ near the peak wavelength to -5.5% in the far wings of the line. Often one fits a polynomial to these data before taking the Abel inversion. For example, we have fit $I(\lambda, X)$ data to the relation[6]

$$I(\lambda, X) = \{\exp[-D(X - X_0]\}[A + B(X - X_0)^2 + C(X - X_0)^4]. \tag{7}$$

We can determine the standard deviation of the coefficients in this relation. A fit to typical (experimental) data of $I(\lambda, X)$ vs X is shown in Fig. 2. Also shown is the best fit to the curve when each coefficient is set at $+\sigma$ and $-\sigma$ from its best-fit value. The corresponding $\overline{I(\lambda, X)}$ vs X curve is also shown in Fig. 2. This wavelength position corresponds to the curve of maximum change in the difference between I and $\bar{I}$. We can carry over data-processing error-bars from this X–Y space into r-space to obtain error-bars in the $I(\lambda, r)$ vs r curve. This procedure is necessary since the half-widths and emissivity are obtained in the radial-space. Figure 3 shows $I(\lambda, r)$ and $\overline{I(\lambda, r)}$

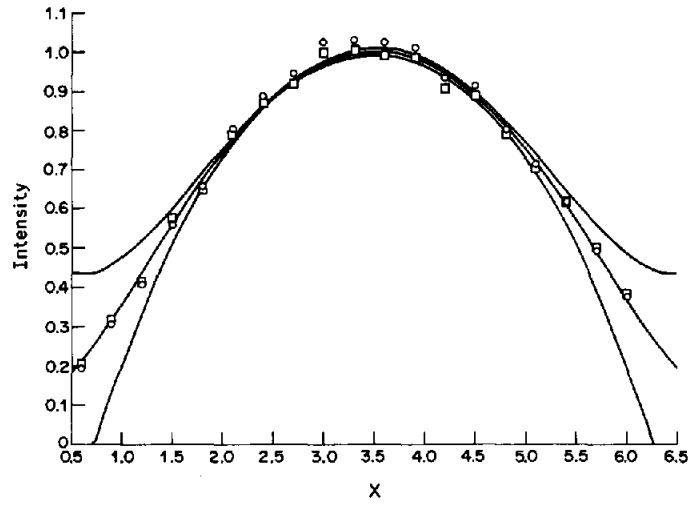

Fig. 2. Typical d.c. intensity vs X data are shown. The average data curve were computer-generated from Eqs. (3)–(5). Also shown is the best fit to the d.c. curve when each coefficient is set at $+\sigma$ and $-\sigma$ from its best-fit value. The wavelength position chosen corresponds to the curve of the maximum difference between I and $\bar{I}$. □—d.c. data; ○—average data.

with error bars. The difference between these two curves is considerably less than the data-processing error bars.

When we integrate over λ [i.e., sum $I(\lambda, X)$ over the 100 λ values] we find a difference of $<0.5\%$ between $I(X)$ and $\overline{I(X)}$ for all values of X. This result is well within the statistical error of most experiments and, hence, we conclude for total emissivity measurements that a relatively large ($\approx 50\%$) a.c. power component has no effect on the data provided we average over the power variation.

We have assumed the line shape to be governed by a Lorentzian curve and that the total emissivity and half-widths are related by Griem's theory[3] and the LTE assumption. We conclude that the time-averaged data over a.c. power variations, when processed by Abel-inversion techniques, give values of $I(r)$ and $\Gamma(r)$ which are the same within data-processing error-bars as the values obtained with the a.c. absent.

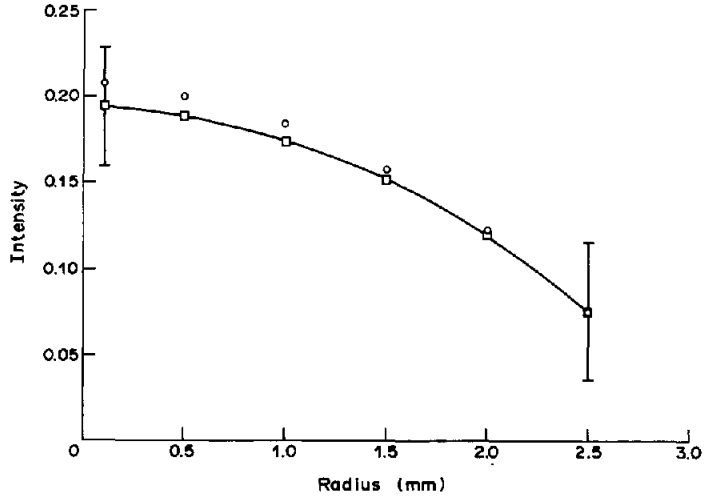

Fig. 3. $I(\lambda, r)$ (d.c. data) and $\overline{I(\lambda, r)}$ (average data) are shown with error bars. The differences between these two curves are considerably less than the data-processing error bars. □—d.c. data; ○—average data.

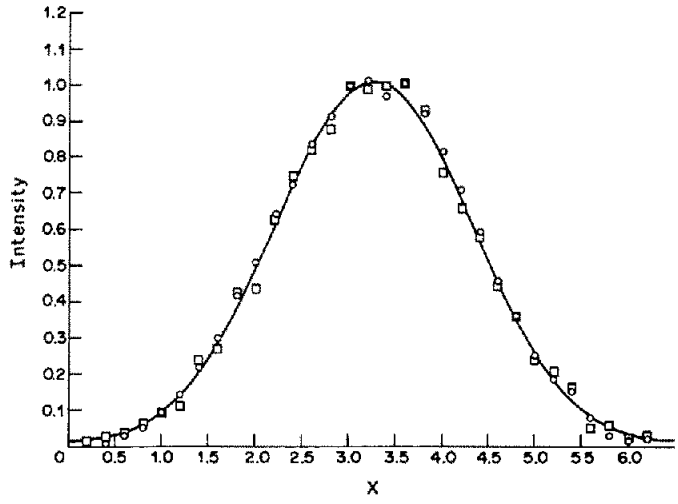

Fig. 4. $I_t(\lambda, X)$ (d.c. data) and $\overline{I(\lambda, X)}$ (average data) are shown vs X near the center wavelength of the H_β transition. The $I_t(\lambda, X)$ curve shown is near its mid-point value and corresponds to d.c. data. □—d.c. data; ○—average data.

EXPERIMENTAL STUDIES

We have also investigated the problem posed by us experimentally and have taken data of $I(\lambda, X, t)$ vs X, λ and t with a pulsed vidicon detector (EG&G Model 1261) at exposure times of 0.5 msec in 0.5 msec step time delays across the 5.56 msec 180 Hz variation of our power supply. We have compared these data with time-averaged data for both the Ar I 4300 Å line and the H_β line. The power-supply variation was approx. 20%.

The difference between $\overline{I(\lambda, X)}$ and $I(\lambda, X, t)$ gets smaller as $I(\lambda, X, t)$ approaches the mean value of its variation. Figure 4 shows the (normalized) $I(\lambda, X, t)$ and $I(\lambda, X)$ data vs X near the center wavelength of the H_β transition for $I(\lambda, X, t)$ near its mid-point values. There is no difference between these two curves when they are fitted to Eq. (6). This result is typical for all values of λ. We obtain similar results when analyzing experimental data for the 4300 Å Ar I transition. These experimental line-shape measurements show that the analysis based on Lorentzian line shapes can be generalized to the more complicated H_β line.

We conclude that emissivity data from a thermal plasma, when processed for either total emissivity or half-width values, are not affected by appreciable a.c. power components if data are averaged over the power variation.

Acknowledgements—The work described in this paper was supported by the U.S. Department of the Interior Bureau of Mines under contract No. J0134035 through Department of Energy under contract number DE-AC07-76ID01570.

REFERENCES

1. "Plasma Technology in Metallurgical Process," Jerome Feinman ed., Iron and Steel Society Inc., 410 Commonwealth Drive, Warrendale, PA (1987).
2. D. W. Jones and W. L. Wiese, *Phys. Rev. A* **34,** 450 (1986).
3. W. L. Wiese, *Plasma Diagnostics Techniques*, R. M. Huddelston and S. L. Leonard eds., Academic Press, New York, NY (1964).
4. H. R. Griem, *Plasma Spectroscopy*, McGraw–Hill, New York, NY (1964).
5. H. R. Griem, *Spectral Line Broadening by Plasma*, Academic Press, New York, NY (1964).
6. V. Bakshi and R. J. Kearney, submitted to *JQSRT* (1989).
7. E. Pfender and M. Boulos, *Thermal Plasmas: Technology and Applications*, Vol. 2, M. I. Boulos ed., Sherbrook, Quebec, Canada (1983).
8. B. S. Choi and H. Kim, *Appl. Spectrosc.* **36,** 71 (1982).